

Energetic-Ion-Driven Global Instabilities Observed in the Large Helical Device and Their Effects on Energetic Ion Confinement

Kazuo TOI

National Institute for Fusion Science, Toki 509-5292, Japan

(Received 23 May 2012 / Accepted 20 August 2012)

This paper reviews various global instabilities destabilized by tangential neutral beam injection (NBI) in the Large Helical Device (LHD) plasmas. These global modes are toroidal Alfvén eigenmodes (TAEs), which are also observed in tokamak plasmas, and helicity-induced Alfvén eigenmodes (HAEs) which are observed only in three-dimensional plasmas such as LHD plasmas. Moreover, reversed magnetic shear Alfvén eigenmodes (RSAEs) are observed in a reversed magnetic shear (RS) plasma in the LHD, where the sign of the magnetic shear changes from positive in the plasma central region to negative in the plasma peripheral region. The RSAEs exhibit a characteristic frequency sweeping due to temporal evolution of the rotational transform profile. In the RS plasma, the energetic-ion-driven geodesic acoustic mode (GAM) is also excited. The GAM interacts nonlinearly with the RSAEs and generates a multitude of frequency sweeping modes through a three-wave-coupling process. The TAEs and GAM exhibit various types of nonlinear evolution, that is, pitchfork splitting and rapid frequency chirp-up and/or chirp-down. The linear and nonlinear characteristics of these energetic-ion-driven global instabilities in the LHD are compared with those observed in tokamak plasmas. TAE bursts having rapid frequency chirp-down induce redistribution and/or loss of energetic ions. Future important issues are briefly described.

© 2013 The Japan Society of Plasma Science and Nuclear Fusion Research

Keywords: alpha particle, energetic ion, helical/stellarator, tokamak, Alfvén eigenmode, rotational transform profile, two-dimensional and three-dimensional plasmas

DOI: 10.1585/pfr.8.1102002

1. Introduction

Energetic alpha particles produced in deuterium-tritium (D-T) reactions and beam ions produced by neutral beam injection (NBI) and/or RF heating play an important role in burning plasmas. Good confinement of these energetic particles is crucial for a magnetic confinement fusion reactor to sustain fusion burning and avoid serious damage of plasma-facing components by energetic ion loss. Alpha particles and beam ions can interact resonantly with magnetohydrodynamic (MHD) waves in the course of slowing down and pitch angle scattering by Coulomb collisions and can destabilize various global instabilities such as Alfvén eigenmodes (AEs). The potential excitation of AEs is often evaluated by two parameters: the volume-averaged beta value of the energetic ion content $\langle\beta_{\text{hot}}\rangle$ and the velocity ratio v_{hot}/v_A , where v_{hot} and v_A are the average velocity of energetic ions over the distribution function and the Alfvén speed, respectively. In a tokamak-type reactor such as the International Thermonuclear Experimental Reactor (ITER), $\langle\beta_{\text{hot}}\rangle \approx 0.3\%$ and $v_{\text{hot}}(0)/v_A(0) \approx 1.9$ are expected [1]. AEs may be destabilized and would enhance radial redistribution and/or loss of energetic alphas and beam ions. The characteristics of energetic-ion-driven AEs and their impacts on energetic-ion confinement have been intensively investigated in major tokamaks [1]. On

the other hand, a helical/stellarator-type reactor, for instance, ARIES CS [2], is being designed on the basis of an operation scenario with high-density ($\sim 5 \times 10^{20} \text{ m}^{-3}$) and relatively low-temperature (volume-averaged temperature of $\sim 7 \text{ keV}$) plasmas in which the slowing-down time of energetic ions and thus $\langle\beta_{\text{hot}}\rangle$ are minimized. Even in the operational scenario, $\langle\beta_{\text{hot}}\rangle \approx 0.2\%$ and $v_{\text{hot}}/v_A \approx 2$ are inferred. Energetic alphas may destabilize AEs in such a helical/stellarator burning plasma. Enhanced energetic ion redistribution and/or losses due to AE excitation are also an important issue for a helical/stellarator reactor.

Comparison studies of AEs and AE-induced effects in tokamak and helical/stellarator plasmas are very effective for a comprehensive understanding of these instabilities and for developing control scenarios for them [3]. The tokamak and helical/stellarator magnetic configurations are clearly different; that is, the former is two-dimensional (2D) and axisymmetric in an ideal case and the latter is three-dimensional (3D). However, a real tokamak plasma appreciably deviates from two dimensions and axisymmetry owing to toroidal field ripple and other 3D effects. Moreover, some differences are present in the rotational transform $\iota/2\pi$ or the safety factor q ($\iota/2\pi = 1/q$) profile and the global magnetic shear profile $s = (\rho/q)dq/d\rho$, as shown in Fig. 1, where ρ denotes the normalized minor radius. In contrast to a standard tokamak plasma, the

author's e-mail: toi@lhd.nifs.ac.jp

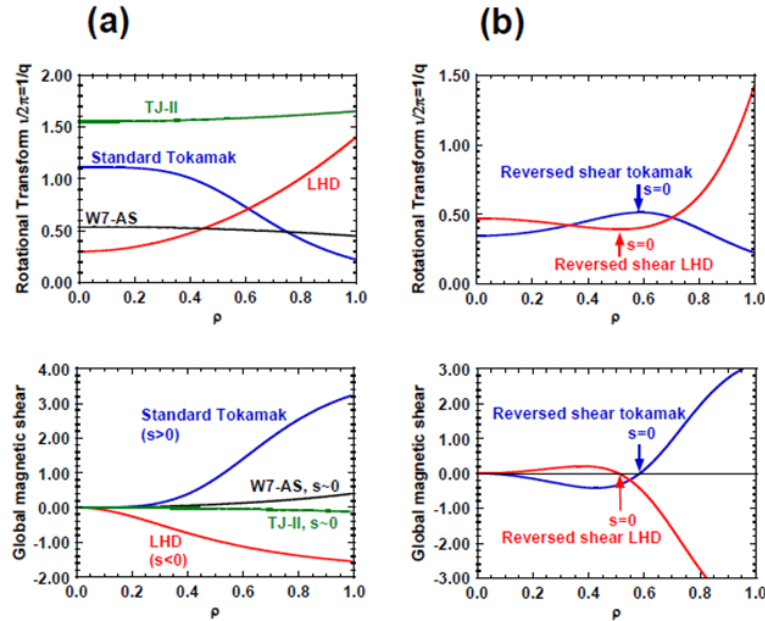


Fig. 1 (a) Monotonic rotational transform (upper frame) and global magnetic shear (lower frame) profiles in a standard tokamak and three typical helical/stellarator devices, LHD, W7-AS and TJ-II. (b) Rotational transform (upper frame) and global magnetic shear (lower frame) profiles in reversed magnetic shear configurations of a tokamak and the LHD.

Large Helical Device (LHD) plasma in low beta (=plasma kinetic pressure/magnetic pressure) regime has finite and negative magnetic shear over the entire region, and W7-AS and TJ-II stellarators have almost no magnetic shear. The magnetic shear in the central region of a reversed magnetic shear (RS) plasma in the LHD has a different sign for that in an RS tokamak.

In this review, energetic-ion-driven global instabilities observed in LHD plasmas heated by tangential neutral beam injection (NBI) are summarized and compared with those in tokamak plasmas. In Sec. 2, shear Alfvén gap formation in an LHD plasma is described. In Sec. 3, possible AEs are calculated for various monotonic $\iota/2\pi$ profiles and are compared with the AEs observed in the LHD. Reversed shear Alfvén eigenmodes (RSAEs) are also observed in a nonmonotonic $\iota/2\pi$ profile, that is, in an RS plasma. A characteristic Alfvén eigenmode in 3D plasmas, the helicity-induced Alfvén eigenmode (HAE), is also detected in LHD plasmas at a lower toroidal magnetic field B_t . Moreover, a peculiar energetic-ion-driven mode having the toroidal mode number $n = 0$, the geodesic acoustic mode (GAM), is observed in LHD plasmas. The linear and nonlinear behaviors of these AEs and GAM are discussed in Sec. 3. Section 4 describes the enhanced radial transport of energetic ions due to toroidal Alfvén eigenmode (TAE) bursts. In Sec. 5, future important issues for comprehensive understanding of global modes destabilized by energetic ions in toroidal plasmas are listed.

2. Shear Alfvén Gap Formation in an LHD Plasma

In an LHD plasma confined in a 3D configuration, both toroidal and poloidal mode coupling play an essential role in gap formation in the shear Alfvén spectra. In toroidal mode coupling, Fourier modes having the toroidal mode number $n = n_1$ can couple with the Fourier modes having different $n = n_2$, provided that $n_1 \pm n_2 = kN$, where N is the toroidal period number and $k = 0, 1, 2, \dots$. These modes form the mode family of $n = n_1$. The number of the mode family is finite, $1 + N/2$ [4]. Coupling occurs among all modes belonging to the mode family of $n = n_1$ and generates new spectral gaps such as HAE gaps in addition to the usual TAE and other axisymmetric gaps, which are formed only by poloidal mode coupling.

The magnetic field strength on the magnetic surface ψ of a 3D plasma is expressed as

$$B/B_0 = 1 + \sum_{\mu,\nu} \varepsilon_B^{\mu,\nu}(\psi) \cos(\mu\theta - \nu N\phi). \quad (1)$$

Here, Boozer coordinates (ψ, θ, ϕ) are used. The parameters μ and ν are integers. B_0 is the averaged field strength, and $\varepsilon_B^{\mu,\nu}$ is the amplitude of each Fourier component. Various spectral gaps are generated as adjacent Alfvén branches intersect, that is,

$$\omega = k_{||m,n} v_A = -k_{||m+\mu, n+\nu N} v_A. \quad (2)$$

The numbers m and n are the poloidal and toroidal mode numbers, respectively. From this equation, the gap frequency is expressed as follows [5–7]:

$$f^{\mu,\nu} = |\nu q^* N - \mu| \left(\frac{v_A}{4\pi R q^*} \right). \quad (3)$$

Here, R is the major radius. The q value at the crossing point, q^* , is expressed as

$$q^* = \frac{2m + \mu}{2n + \nu N}. \quad (4)$$

The expressions for 2D plasmas correspond to those with $\nu = 0$. As seen from Eq. (2), toroidal mode coupling disappears for a 2D plasma, i.e., $\nu = 0$. The TAE corresponds to the case of $\mu = 1$, $\nu = 0$, and the ellipticity-induced Alfvén eigenmode (EAE) corresponds to $\mu = 2$, $\nu = 0$. The Alfvén eigenmode induced by the helical component, $\cos(2\theta - N\phi)$, corresponds to $\mu = 2$, $\nu = 1$, which is termed an HAE₂₁ and is simply referred to as an HAE here [5–7]. As seen from Eq. (3), the HAE frequency for the dominant helical component $\cos(2\theta - N\phi)$ in an LHD plasma with $N = 10$ is greater than the TAE frequency by approximately a factor of N . Obviously, toroidal mode coupling is essential to generate the HAE gap due to $\nu \neq 0$. Note that the gap width is approximately proportional to the amplitude of the relevant Fourier component $\varepsilon_B^{\mu,\nu}$ and the mode frequency. The HAE gap can usually be much wider than the TAE gap for helical/stellarator devices with a large N such as in the case of the LHD ($N = 10$). The resonance condition between passing energetic ions and AEs is expressed as [6]

$$v_{b\parallel} / v_A = \frac{1}{1 \pm 2/(\nu N q^* - \mu)}, \quad (5)$$

where $v_{b\parallel}$ is the parallel velocity of the passing energetic ions. The resonance condition for TAE ($\mu = 1$, $\nu = 0$) is $v_{b\parallel} / v_A = 1$ (fundamental excitation) and $v_{b\parallel} / v_A = 1/3$ (sideband excitation). That for an HAE in the LHD is similar to the fundamental excitation of the TAE, i.e., $v_{b\parallel} / v_A \sim 1$.

In LHD plasmas with a large N ($=10$), the effect of toroidal mode coupling on the eigenfrequency of TAEs is small, typically less than 10% [8]. This was first confirmed in the analyses of the Compact Helical System (CHS), which is a smaller version of the LHD with $N = 8$ [9]. Moreover, the eigenfunction of the TAE is determined by the fundamental toroidal mode number and is scarcely affected by toroidal mode coupling [8,9]. An example in the LHD is shown in Fig. 2 [8]. In the figure, the shear Alfvén spectra are shifted slightly downward by including toroidal mode coupling but the eigenfunction remains unchanged. That is, in helical/stellarator plasmas with $N \gg 1$, TAEs, EAEs, global Alfvén eigenmodes (GAEs), and RSAEs are essentially the same as those in tokamak plasmas. The characteristics of these AEs do not depend on 3D toroidal configuration effect. The increase in the TAE gap frequency toward the edge is due to the shape of the rotational transform $\iota/2\pi$ ($=1/q$) profile. The stability of these AEs is determined by a competition between the energetic ion drive and various damping mechanisms due to background plasma such as continuum damping [10–12]. In a low-beta LHD plasma with negative magnetic shear over the entire

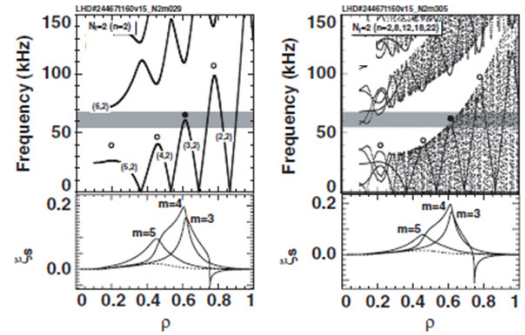


Fig. 2 Comparisons of shear Alfvén spectra and TAE eigenfunctions in two cases without (left frames) and with (right frames) toroidal mode coupling (see [8] for details).

plasma region, as shown in Fig. 1 (a), continuum damping plays an important role because the TAE gaps are not well aligned from the plasma core to the edge.

3. Energetic-Ion-Driven Global Instabilities Observed in LHD Plasmas

Energetic-ion-driven AEs have been reported in several helical/stellarator devices. Among those devices, the CHS and LHD have appreciable magnetic shear, the magnitude of which is comparable to that in tokamaks. Moreover, the high $\iota/2\pi$ (or low q) region, including the $\iota/2\pi = 1$ surface, in the monotonic profiles is located at the edge of LHD plasmas, whereas it is in the central region of the tokamak profile (Fig. 1 (a)). Reversed shear profiles are generated in both LHD and tokamak plasmas but have opposite signs of the global magnetic shear in the central plasma region (Fig. 1 (b)). Another type of helical/stellarator device is a shearless stellarator such as W7-AS or TJ-II, as shown in Fig. 1 (a). Moreover, the GAM or high-frequency zonal flow having an $n = 0$ mode structure is also destabilized by energetic ions in LHD and tokamak plasmas and is a global mode that differs from that excited through nonlinear coupling of drift waves. These AEs and the GAM sometimes interact and excite other modes through three-wave coupling. Moreover, they exhibit interesting nonlinear behaviors that reflect nonlinear interaction between the mode and energetic ions in phase space.

3.1 AEs in plasmas with a monotonic rotational transform profile

We calculated the shear Alfvén spectra and AEs for various model rotational transform profiles that can be formed in the LHD by increasing the averaged toroidal beta values [3]. The calculation showed that GAEs and RSAEs as well as TAEs can be excited in the LHD. Here, toroidal mode coupling was not considered because it does not obviously affect these AEs in LHD plasmas with a large N ($= 10$), as mentioned above. The possible $\iota/2\pi$ profiles in the LHD are not usually realized in a standard toka-

mak plasma but may be realized by a local current drive using electron cyclotron waves, a strong edge bootstrap current, sawtooth crash, or other effects.

In a low-beta LHD plasma, where pure hydrogen plasma with a line-averaged electron density of $1 \times 10^{19} \text{m}^{-3}$ is assumed at a toroidal magnetic field of 1 T, the $n = 1$ TAE gap is formed by the coupling of $m = 2$ and $m = 3$ in the plasma central region with low magnetic shear (Fig. 3 (a)). The major and averaged minor radii of the plasma are assumed to be $R \approx 3.67 \text{ m}$ and $a \approx 0.64 \text{ m}$, respectively. Two types of core-localized TAEs (C-TAEs), which are composed of two dominant Fourier components, $m = 2$ and $m = 3$, exist in the gap. The lower-frequency mode has *even* radial parity, where two Fourier components have the same polarity in the larger major radius side (i.e., the outboard side of a toroidal plasma), whereas the higher-frequency one has *odd* radial parity. Here these eigenfunctions are calculated by the AE3D code [13]. The lower-frequency and higher-frequency modes are thought to have ballooning and anti-ballooning characteristics, respectively, as is the case in tokamaks. Note that the sharp discontinuity in the $m = 2$ Fourier component shown in Fig. 3 (b) is caused by the singularity of the ideal MHD equations coming from the Alfvén resonance, which would lead to appreciable continuum damping. C-TAEs were first observed in the CHS with $N = 8$ [9, 14]. Subsequently, these TAEs were also observed in the LHD [8, 15]. Two C-TAEs having a frequency separation corresponding to the predicted TAE gap width were detected in the shot. These TAEs are thought to be even- and odd-parity C-TAEs for the lower- and higher-frequency modes, respectively. This

was confirmed theoretically [16]. The C-TAE with even parity was preferentially observed in tokamaks [17–19]. The C-TAE with odd parity was also observed later in the Joint European Torus (JET) [20]. Note that AE studies in the LHD are conducted at a lower toroidal field (typically less than 1.5 T), and the toroidal rotation velocity is less than 20 km/s on the magnetic axis. Accordingly, the Doppler effect on the AE frequency is small for the low- n AEs observed in LHD plasmas.

When the plasma beta is increased slightly in an LHD plasma, the $n = 1$ TAE gap formed by poloidal coupling of the $m = 2$ and $m = 3$ modes disappears from the central plasma region due to the increase in the rotational transform there. In this region (normalized minor radius $\rho < 0.5$), GAEs whose frequencies are just above the maximum of the continuum and below the minimum are found by the AE3D code, as shown in Fig. 4 (a). The GAE existing just above the maximum of the continuum is sometimes called a nonconventional GAE [21]. The calculated eigenfunction of the GAE at 33.0 kHz is composed of a single Fourier mode, $m = 2/n = 1$, and the radial mode number is $p = 0$, as shown in Fig. 4 (b). The other GAE at 30.6 kHz, which is closer to the continuum, has the radial mode number $p = 1$. GAEs are also found in the region just below the continuum where $m = 3/n = 1$, as shown in Fig. 4 (c), where four GAEs were found. As the frequency of GAEs approaches the minimum of the continuum, the radial mode number of the eigenfunction increases from $p = 0$ to $p = 2$ in this case. Although the eigenfunction of the $m = 2$ or $m = 3$ mode with $p = 0$ has a broader mode structure, the eigenmodes having higher p values ($=1$ or 2)

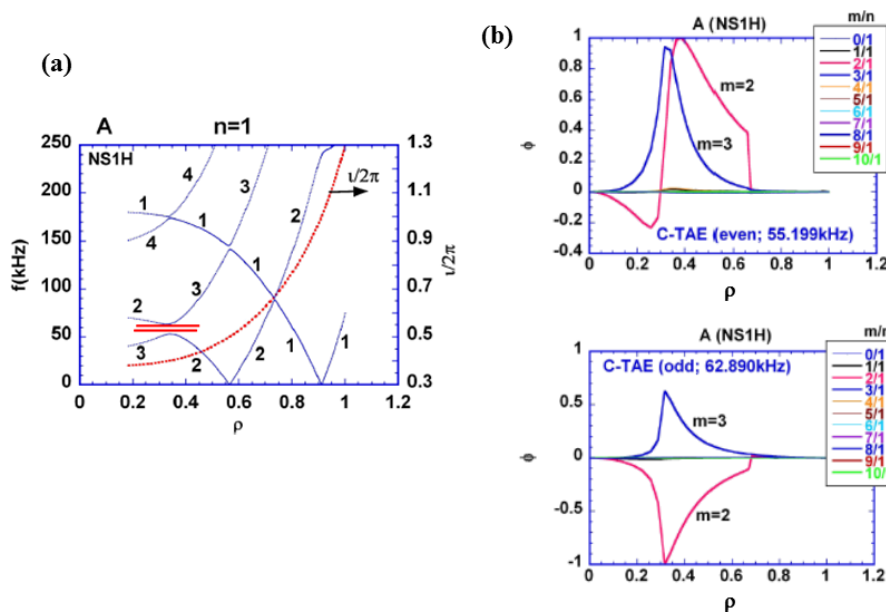


Fig. 3 (a) Shear Alfvén spectra ($n = 1$) and rotational transform profile in a low-beta LHD plasma. The two horizontal bars denote the eigenvalues of TAEs. (b) Eigenfunctions of *even*- and *odd*-parity core-localized TAEs, corresponding to the two eigenvalues. (See [3] for details.)

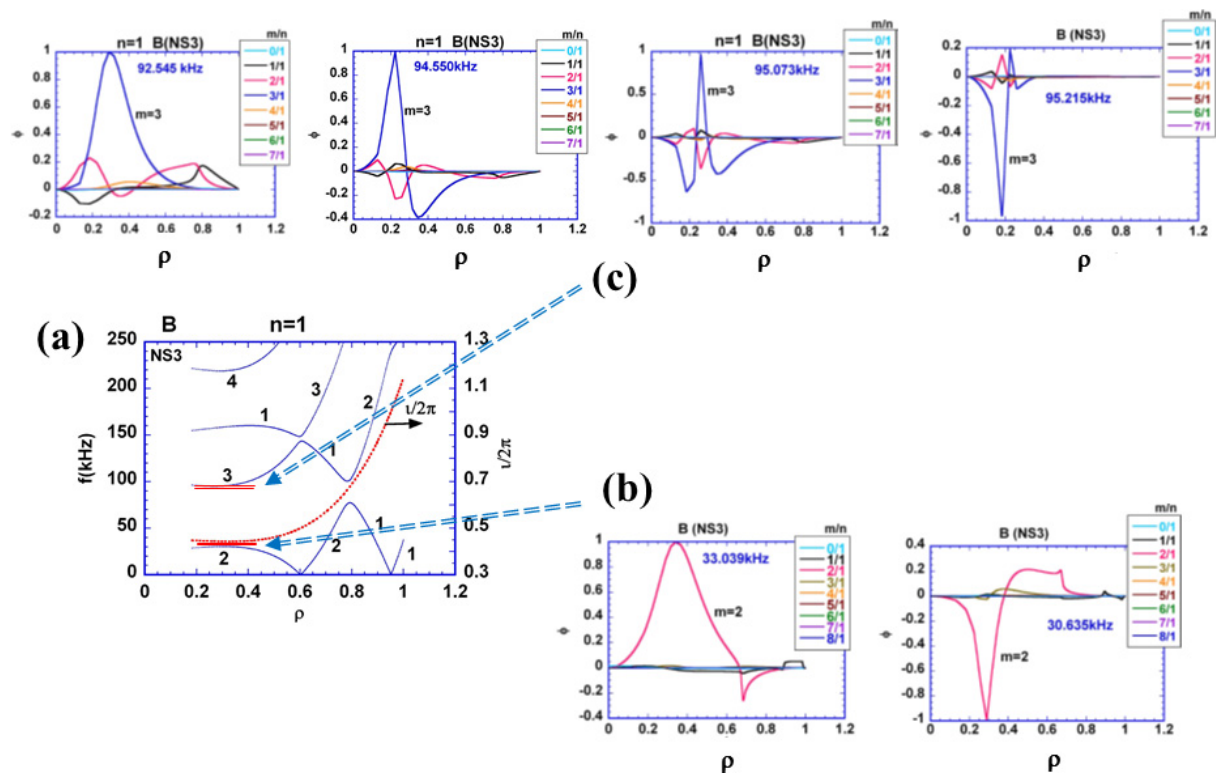


Fig. 4 (a) Shear Alfvén spectra ($n = 1$) and rotational transform profile in an LHD plasma with slightly increased beta. Horizontal bars denote the eigenvalues of GAEs. (b) GAEs located just above the continuum, where they have different radial mode numbers, (c) GAEs located just below the continuum, which have different radial mode numbers. (See [3] for details.)

are localized more strongly around the minimum or maximum of the continuum and have a more prominent RSAE-like localized character [3]. This indicates that the RSAE can reside even in a monotonic rotational transform profile having an appreciably low shear zone in the plasma core as well as in an RS plasma [22]. The determination of which modes having different radial mode number p are the most unstable will depend on the plasma parameters and radial profiles such as the $u/2\pi$ profile and energetic ion pressure profile.

In the LHD, the transition from the TAE to the GAE, which is due to the evolution from the case shown in Fig. 3 to that in Fig. 4, often occurs because of the increase in the rotational transform near the center caused by the Shafranov shift and/or co-current drive by NBI [8, 15]. Note that the co-current driven by NBI increases the external rotational transform produced by helical coils. In this situation, the $n = 1$ TAE gap formed by $m = 2$ and $m = 3$ mode coupling is removed from the plasma region. After the transition, GAEs can be excited by energetic ions in the plasma core region.

3.2 AEs in reversed magnetic shear plasmas

In RS tokamak plasmas, characteristic energetic-ion-driven modes called RSAEs or Alfvén cascade modes are observed [23–31]. Moreover, a GAM having an $n = 0$ mode structure is sometimes excited by energetic ions

[32, 33]. A theoretical interpretation of recent observations in DIII-D was attempted [34]. The excitation of RSAEs localized around the zero-shear layer ($\rho = \rho_o$) or the location of $q(\rho_o) = q_{\min}$ is determined by the contributions from energetic ions and the gradient of the bulk plasma pressure, which depend on the sign of $q''(\rho_o)$, the fast ion density gradient, the normal curvature of the magnetic field structure, and other factors [22, 23, 35, 36]. As illustrated in Fig. 1 (b), the RS configurations in tokamak and LHD plasmas have opposite signs for the curvature of the q profile at the zero-shear layer, i.e., $q''(\rho_o) > 0$ in tokamaks and $q''(\rho_o) < 0$ in the LHD. It is interesting and important to investigate how the frequency of the RSAE behaves in these RS plasmas having different signs of $q''(\rho_o)$ at the zero-shear layer.

A large Shafranov shift is induced in high-beta LHD plasmas and generates RS plasmas. In the LHD, the RS configuration is also produced by off-axis counter neutral-beam current drive (NBCD). In this case, the energetic ion contribution is significant. Figure 5 (a) shows a typical time evolution of the electron temperature measured at various radial locations with an electron cyclotron emission (ECE) diagnostic, together with those of the line-averaged electron density and plasma current induced by NBCD. Spectrograms of the magnetic probe and microwave interferometer signals are also shown in Fig. 5 (b) [37]. The minimum of the rotational transform $(u/2\pi)_{\min} (=q_{\max})$ in

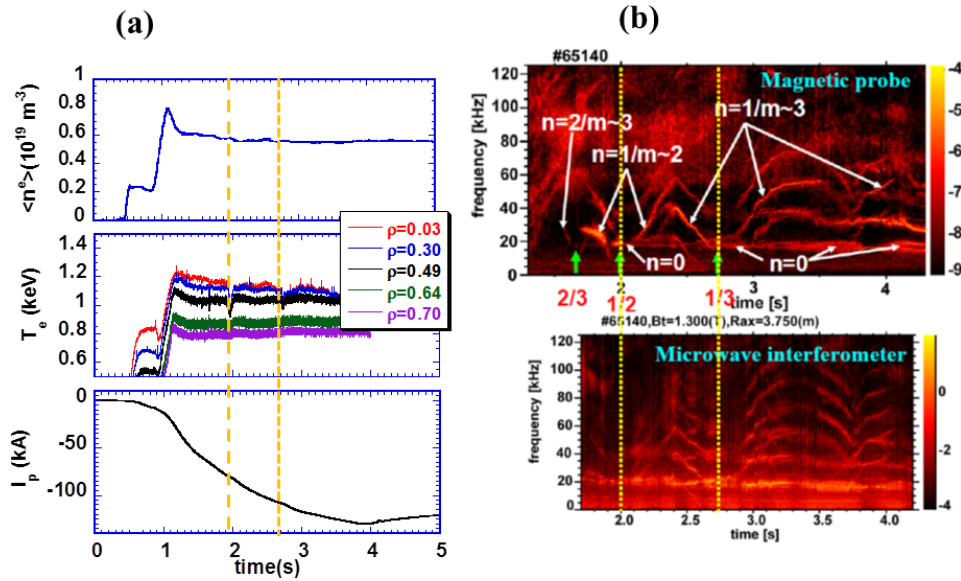


Fig. 5 (a) Waveforms of line-averaged electron density, electron temperature derived from ECE signals, and plasma current, (b) spectrograms of the magnetic probe and 2-mm microwave interferometer signals. (See [37] for details.)

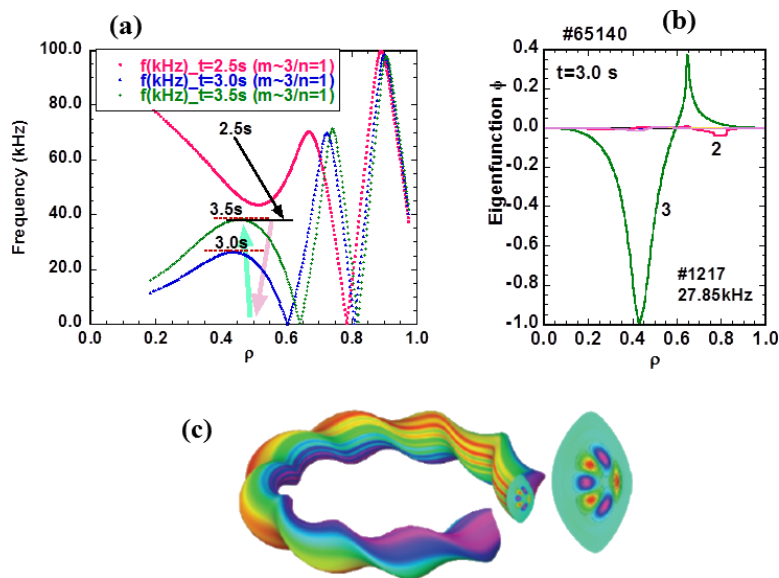


Fig. 6 (a) Shear Alfvén spectra at three time slices in the RS plasma shown in Fig. 5, (b) eigenfunction of the RSAE at $t = 3.0\text{ s}$ calculated by the AE3D code, and (c) 3D variation in the $m = 3/n = 1$ RSAE on the outer flux surface of the LHD and the mode pattern in the cross section. (See [37, 41] for details.)

the RS plasma evolves in time through the rational values $2/3$, $1/2$, and $1/3$ as the NB-driven current rises in the counter direction. The ECE signals at the plasma core region exhibit sharp dips when $(l/2\pi)_{\min}$ or q_{\max} has passed these rational values. The rotational transform profile measured by motional Stark effect spectroscopy also indicated the formation of an RS profile with a minimum around $\rho = 0.4$ to 0.5 [37]. During the rise in the counter plasma current, a characteristic “symmetric” frequency sweeping from downward to upward via the minimum frequency was observed, while the line-averaged electron density was

kept constant [37–40]. The mode numbers derived from the magnetic fluctuation signals are shown in Fig. 5(b). These modes were identified as RSAEs by comparing these data with the eigenmode frequencies and eigenfunctions calculated by the AE3D code [13]. The eigenvalue at $t = 2.5\text{ s}$ was found just below the shear Alfvén continua, and the eigenvalues at $t = 3.0\text{ s}$ and 3.5 s were found just above the continua. The RSAEs are excited in RS plasmas produced by counter NBI alone. These eigenvalues correspond to an RSAE whose eigenfunction consists of a single dominant component of $m = 3/n = 1$ and is localized

around the minimum or maximum of the shear Alfvén continua, that is, near the zero-shear layer (Fig. 6) [37,41]. The time at which the RSAE frequency reaches a minimum indicates that $(t/2\pi)_{\min}$ passed the rational values $(t/2\pi)_{\min} = 1/2$ at $t \approx 2.0$ s and $1/3$ at $t = 2.7$ s. The RSAEs are also detected by a microwave reflectometer/interferometer system, as shown in Fig. 5 (b). When $(t/2\pi)_{\min}$ takes the rational values, the geodesic curvature and pressure gradient effects should be considered in the RSAE dispersion relation. The dispersion indicates that the shear Alfvén continua are bounded by a finite value of $\omega_G^2 + \omega_V^2$. Here, ω_G is the GAM angular frequency. The quantity ω_V^2 is determined by the effective angular frequency offset due to the gradients in the bulk plasma pressure and energetic ion density. In the shot shown in Fig. 5 (b), a peculiar mode having $n = 0$ is also observed in the signals of the magnetic probes and interferometer/reflectometer, together with the RSAE [37, 40]. The observed frequency agrees well with the GAM frequency evaluated at the zero-shear layer using the expression for a helical plasma [42, 43]. This $n = 0$ mode is thought to be the energetic-ion-driven GAM.

RSAs and characteristic frequency sweeping were observed in many tokamaks during ion cyclotron resonance frequency (ICRF) heating and NBI in the current ramp-up phase [23–31]. The RSAE frequency is swept unidirectionally, that is, upward from a certain minimum when q_{\min} decreases in time from a rational value. This frequency sweeping phenomenon was interpreted by including the energetic ion content, toroidal effect, plasma pressure gradient, and other factors. The two dominant contributions, from fast ion effects and the bulk pressure gradient, drive upward sweeping but impede downward sweeping in RS tokamak plasmas [22, 23, 35, 36]. However, in the LHD, downward sweeping is driven mainly by the fast ion effect, and upward sweeping is driven by the pressure gradient effect [37]. The fact that the observed RSAE is a negative frequency mode propagating in the electron diamagnetic drift direction is essential to the above-mentioned “symmetric sweeping” of the frequency. The negative frequency mode can be excited when the energetic ion distribution function is anisotropic [44].

3.3 AEs excited by 3D effect

HAEs exist only in 3D plasmas, and the spectral gap is formed by toroidal mode coupling as well as poloidal mode coupling. An HAE was detected in NBI-heated plasmas in the LHD at a low toroidal field [45]. The HAE frequency is higher than the TAE frequency by approximately a factor of N , as discussed in Sec. 2, which corresponds to the frequency range of 200 kHz to 300 kHz at $B_t = 0.5$ T in hydrogen plasmas having an electron density of $1\text{--}2 \times 10^{19} \text{ m}^{-3}$. The spectrogram and amplitude of the magnetic probe signal are shown in Figs. 7 (a)-(c). At $t \approx 1.5$ s, coherent modes are found at ~ 200 kHz together with the mode at $f = 30\text{--}40$ kHz, which is a TAE.

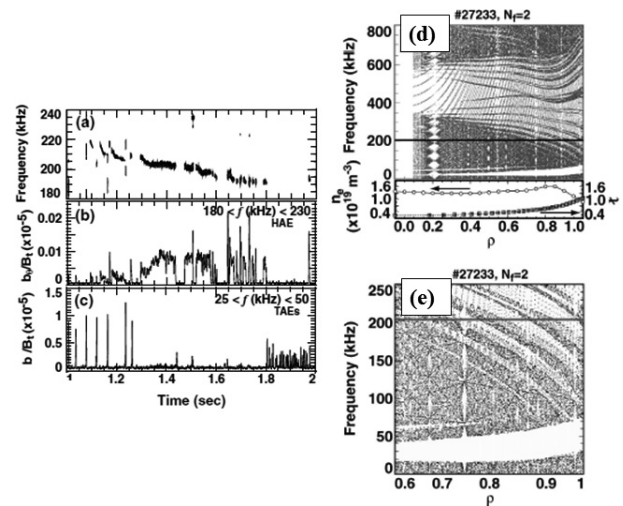


Fig. 7 Observed magnetic fluctuations associated with HAE ((a) and (b)) and TAE (c) in the LHD, (d) and (e) HAE gap calculated for an LHD plasma at a low toroidal field. (See [45] for details.)

The higher-frequency mode is an HAE. The toroidal mode number was $n = 2$ in this shot. The shear Alfvén spectra was calculated, including toroidal mode coupling among Fourier modes in the $n = 2$ mode family, as shown in Figs. 7 (d) and (e). The center of a very wide gap appears around 450 kHz. From the analytic Eq. (3) of the HAE gap frequency, the HAE gap center is estimated as ~ 480 kHz, assuming $q^* \approx 1$. This very wide gap appears only in the calculation when toroidal mode coupling is considered. In conclusion, this gap is the HAE gap. From the observed mode frequency, the HAE is thought to exist near the plasma peripheral region of $0.7 < \rho < 1$. In the plasma at low B_t ($=0.5\text{--}0.6$ T), the orbits of passing ~ 180 keV energetic ions considerably deviate outward from the magnetic surfaces. This leads to a large energetic ion pressure gradient near the edge, which would destabilize HAEs near the plasma edge. This prediction that the energetic ion pressure profile has a steep gradient near the plasma edge at low B_t was confirmed by a numerical calculation of the deposition profile of injected beam ions [46]. Several continuous spectra extending from the core to the edge inside the HAE gap are generated by the deviation from the helical symmetry. The many upward curves inside the HAE gap indicate the continua that remain because the counterparts to be coupled are missing, where only a finite number of modes (915 modes) were included in the calculation. The amplitude of the observed HAE is fairly weak, and no visible effect on energetic ion transport was observed. The density fluctuations driven by the HAE were observed recently using a fast response H α detector array. The radial profile of the coherence between each H α detector and the magnetic probe signals showed a peak near the plasma edge where the relevant HAE gap exists [3].

A real tokamak is no longer a 2D system because of

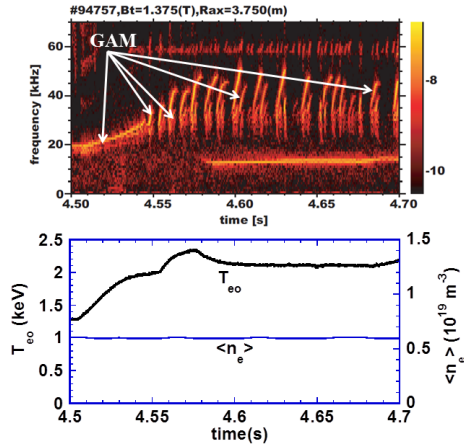


Fig. 8 Spectrogram of magnetic fluctuations induced by GAM during ECH in an RS plasma produced by counter NBCD and time evolution of the electron temperature near the plasma center ($\rho \sim 0.2$) and line-averaged electron density, where ECH is switched on at $t = 4.5$ s.

several 3D factors: magnetic field ripple, resonant magnetic perturbations, and helical deformations due to large-scale MHD instabilities such as the resistive wall mode. In such cases, the toroidal field period number N is low, typically 1 or 2. In such low- N 3D configurations, the shear Alfvén spectra and gap formation will be considerably modified by the rather strong toroidal mode coupling.

3.4 Energetic-ion-driven geodesic acoustic modes

The GAM, which is a type of zonal flow, can be excited by energetic ions in RS tokamaks [32, 33]. This energetic-ion-driven GAM, together with RSAEs, was also observed in RS plasmas in the LHD, as shown in Fig. 5 (b) [37]. The mode frequency agrees well with that of the GAM and was identified as the energetic-ion-driven GAM. Many frequency-sweeping modes are generated through nonlinear mode coupling between the energetic-ion-driven GAM and RSAEs [37, 40]. The mode frequency clearly increases with the electron temperature by electron cyclotron heating (ECH), as shown in Fig. 8. In this shot, the mode frequency of the GAM increased with time, having a continuous mode character, and then rapidly chirped upward and downward. The energetic-ion-driven GAM induces large potential fluctuations and is also accompanied by appreciable magnetic fluctuations, typically $b_{\theta}/B_t \approx 0.4 \times 10^{-5}$ [40, 47]. In some RS plasmas, the density and potential fluctuations were measured by a heavy-ion beam probe. The root mean square amplitudes of the density and potential fluctuations in the central plasma region (normalized minor radius $\rho < 0.2$) are very large; that is, $(\delta n_e)_{\text{rms}}/n_e$ reaches $\sim 10\%$, and $(\delta\phi)_{\text{rms}}/T_e$ reaches $\sim 100\%$ [47]. An energetic-ion-driven GAM having frequent bursting characteristics was also observed in a monotonic $\iota/2\pi$ profile at very low density ($\leq 1 \times 10^{18} \text{ m}^{-3}$), where the

slowing down time is much longer than the energy confinement time of bulk plasma; that is, the beam beta is much higher than the bulk plasma beta. Extremely large potential fluctuations in the GAM and the radial profile were measured by a heavy-ion beam probe technique [48, 49]. The possibility of bulk ion heating by GAM bursts is under discussion [50]. Note that the energy transfer from energetic particles to waves is proportional to $(\omega \partial f / \partial W + n \partial f / \partial P_{\varphi})$ in a tokamak plasma, where ω , n , f , W , and P_{φ} are the mode angular frequency, toroidal mode number, energetic particle distribution function, particle energy, and canonical angular momentum, respectively [51, 52]. The first term, $\omega \partial f / \partial W$, is related to the gradient or anisotropy of the distribution function in velocity space, and the second is the driving term due to the radial gradient of the energetic particle density. Accordingly, the modes with $n = 0$, such as the energetic-ion-driven GAM, are destabilized by the gradient in velocity space. The destabilization mechanism can also be applied to helical/stellarator plasmas, but only for well-circulating particles in 3D plasmas with large N , where P_{φ} is approximately conserved [52]. This condition is roughly satisfied for energetic ions produced by tangential NBI in LHD plasmas.

3.5 Nonlinear evolution of energetic-ion-driven modes

In the above subsections, the linear behaviors of various Alfvén eigenmodes in the LHD are discussed and compared with those in tokamaks. The nonlinear evolution of AEs is determined by an interaction between the wave field of AEs and the energetic ion distribution function established by the relaxation processes, which tend to restore the unstable distribution function against collisions with the bulk plasma. Two important relaxation processes are the velocity space diffusion caused by ICRF heating (or quasi-linear RF diffusion) and the dynamical friction (or electron drag) for NBI-produced energetic ions. On the other hand, the wave field of the AEs will be controlled by both the energetic ion drive γ_L and damping rate γ_d . The nonlinear evolution of AEs was first investigated by a theoretical model of the bump-on tail instability in which the relaxation process is simulated by the Krook operator [53]. If the annihilation expressed by the Krook operator or quasi-linear diffusion acts as the dominant relaxation process for the energetic-ion distribution function, all types of nonlinear evolution of AEs, that is, (i) a steady-state regime, (ii) a regime with periodic amplitude modulation (or pitchfork splitting), (iii) a chaotic regime, and (iv) an explosive regime having rapid frequency chirping, were theoretically predicted to be possible [53], and the first three regimes were observed in ICRF-heated plasmas in the JET tokamak [54, 55]. However, if the electron drag is the dominant relaxation process, i.e., $E_{\text{in}} \gg E_A \gg E_{\text{crit}}$, only the explosive regime is predicted theoretically, and experimental data from the MAST spherical torus and JET are consistent with the theory [56]. Here, E_{in} , E_A , and E_{crit} are

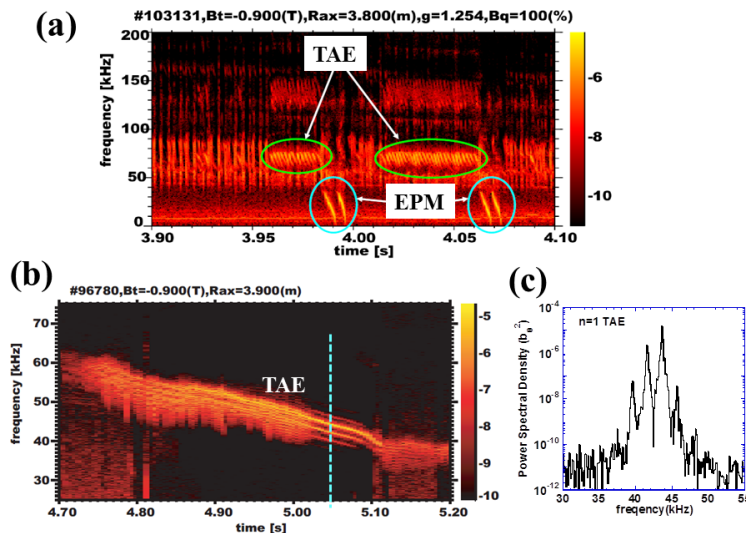


Fig. 9 Nonlinear evolution of TAE and EPM with spectrogram of magnetic probe signal. (a) $n = 1$ TAE and $n = 2$ EPM exhibiting rapid frequency down chirping, and (b) $n = 1$ TAE exhibiting pitchfork splitting of the frequency spectrum into several spectral peaks with equal spacing. (c) Power spectral density of the TAE magnetic fluctuations with pitchfork splitting in the time window from $t = 5.053$ s to 5.057 s, which is indicated by a dotted vertical line in (b).

the initial beam energy, beam energy in the resonance region with AEs, and critical energy of beam heating, respectively. The nonlinear evolution of AEs is determined by the phase space evolution and would be insensitive to the detailed magnetic configuration. Accordingly, it will not have any essential differences in tokamak and helical/stellarator plasmas. Figure 9 shows typical examples of the nonlinear evolution of TAEs and the energetic particle mode (EPM) observed in the LHD. TAEs having rapid frequency down chirping are often observed in NBI-heated plasmas, as shown in Fig. 9 (a), which is consistent with the theory [56]. However, in some outward-shifted plasmas heated by NBI, the $n = 1$ TAE exhibited pitchfork splitting, as shown in Fig. 9 (b). The TAE is composed of two dominant Fourier modes, $m = 1$ and $m = 2$, with their peaks around $\rho \approx 0.7$. In this plasma, electron drag is the dominant relaxation process because $E_{in} \gg E_A \gg E_{crit}$. So far, the theory does not seem to provide a straightforward explanation of this result. As shown in Figs. 5 (b) and 8, the energetic-ion-driven GAM also exhibits pitchfork splitting and rapid frequency chirping in LHD plasmas. Understanding of the nonlinear evolution of AEs and the GAM may provide important information on the energetic ion distribution function.

4. Effects of TAEs on Energetic Ion Transport in LHD

Clump–hole pair formation in phase space that reflects nonlinear wave–particle interactions was investigated with a neutral particle energy analyzer (NPA) with a typical time resolution of 0.5 ms in high-beta LHD plasmas (Fig. 10). The NPA data clearly indicated the formation of clump–

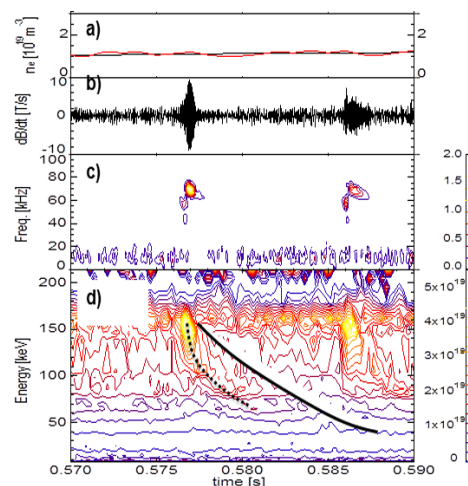


Fig. 10 Clump and hole formation in the energy spectra obtained by NPA in a high-beta LHD plasma. (a) Line-averaged electron density, (b) TAE burst detected by a magnetic probe, (c) spectrogram of the magnetic probe signal, and (d) time evolution of energy spectra of charge-exchange neutral particles. The dotted and solid curves in (d) show the temporal energy decay of the formed clump and hole, respectively. (See [57, 58] for details.)

hole pairs in phase space induced by an $n = 1/m = 1 + 2$ TAE burst (Figs. 10 (b) and (c)) [57, 58]. Note that the TAE gap is located in the plasma peripheral region ($\rho \approx 0.65$). In Fig. 10 (d), the observed charge-exchange neutral flux of energetic ions is enhanced (reduced) by the TAE burst from the value just before the burst, which corresponds to the formation of a clump (hole). During the TAE burst,

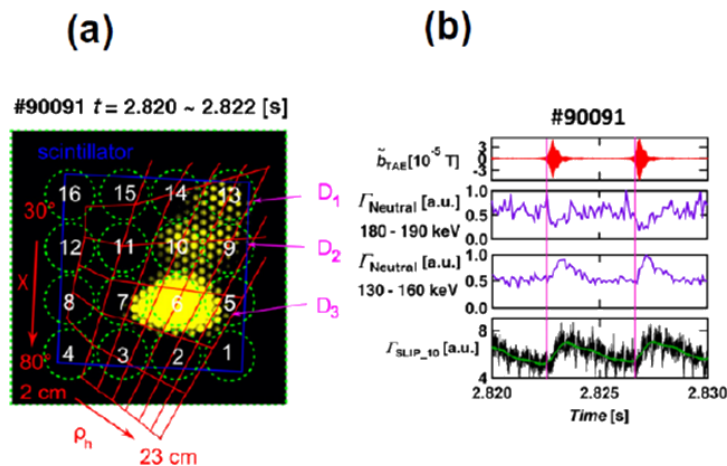


Fig. 11 Energetic ion losses induced by TAE bursts in LHD. (a) Scintillation image captured by a C-MOS camera for a 2 ms exposure time, (b) time evolution of magnetic probe signal of TAE bursts, charge-exchange neutral fluxes measured by NPA, and the SLIP signal in the D_2 domain shown in (a). (See [46] for details.)

the clump energy is quickly reduced from the injection energy to ~ 110 keV within 1 ms. Both the clump and the hole created by the TAE burst exhibit slowing down of the energy with different time scales just after the TAE burst, as shown in Fig. 10(d). From the slowing down time of the hole, the radial location of the hole formed simultaneously with the clump is inferred to be the normalized minor radius $\rho = 0.79$ ($=\rho_{\text{hole}}$). On the other hand, the clump location is inferred to be further outside, $\rho = 0.91$ ($=\rho_{\text{clump}}$). This indicates that energetic ions are transported outward by clump–hole pair formation during the TAE burst by about 10% of the averaged minor plasma radius ($\rho_{\text{clump}} - \rho_{\text{hole}} = \Delta\rho \approx 0.1$). Recently, a new NPA with a fast time response of $10\mu\text{s}$ was developed to clarify the detailed dynamics of this nonlinear process in phase space [59]. The downward frequency chirping of the TAE burst is related to the rapid decrease in the clump energy. The hole is formed near the initial beam energy. A numerical simulation was conducted to analyze the LHD NPA data shown in Fig. 10(d) by using a hybrid code that solves the MHD fluid and drift kinetic equations assuming an axisymmetric equilibrium comparable to that of the LHD [60]. It revealed that the radial excursion of energetic ions by each TAE burst reaches about 10% of the minor radius, as inferred from the experimental data. That is, the radial excursion of energetic ions was obtained when the internal magnetic fluctuation amplitude was assumed to be $\sim 10^{-3}B_t$ (B_t : the toroidal field strength). Comparing the internal TAE amplitude used in the simulation with experimental data is an important issue for future study.

In the LHD, redistribution of energetic ions by TAE bursts is inferred from the NPA data, as discussed above. A fraction of the energetic ions transported outward by TAE bursts are lost, and they are detected by a scintillator-based lost ion probe (SLIP), which can measure the energy and pitch angle of the lost ions simultaneously with high time

resolution. In relatively high-beta plasmas produced in an inward-shifted configuration ($R_{\text{ax}} = 3.6$ m in the vacuum field), TAE-induced energetic ion losses were measured by a SLIP [46]. The energetic passing ions lost in the TAE burst were mostly in the energy ranges $E = 50$ – 150 keV at a pitch angle $\chi \approx 35^\circ$ – 45° . The energy resolution of the SLIP is determined by a simple double aperture structure and is not very good ($\Delta E/E \approx 0.25$ at $E = 150$ keV and $\chi = 60^\circ$). On the other hand, the pitch angle resolution, which is determined mainly by the width of the aperture, is fairly good ($\sim 5^\circ$). The light spots on the scintillator screen representing lost energetic ions are shown in Fig. 11(a) [46]. The dominant losses of energetic ions are observed in three domains: D_1 , D_2 , and D_3 . The spots D_1 , D_2 , and D_3 correspond to dominant losses due to resistive interchange modes excited near the plasma edge, TAE bursts, and collisional ripple transport, respectively. Figure 11(b) shows the time evolution of magnetic fluctuations of the TAE, the charge-exchanged neutral flux ($E = 180$ – 190 keV) measured by the NPA, the flux of slightly slowed-down neutrals ($E = 130$ – 160 keV), and the loss flux of energetic ions measured by the SLIP in domain D_2 . The ion flux having the injection beam energy $E = 180$ – 190 keV shows a sharp drop and slow recovery. The neutral flux from slightly slowed-down ions ($E = 130$ – 160 keV) shows a rapid rise and slow decay. As discussed regarding Fig. 10, these signals indicate that the hole is formed around the injection energy, and the clump is observed in the energy range $E = 130$ – 160 keV. The SLIP signal has almost the same or a slightly slower rise than the NPA flux ($E = 130$ – 160 keV). This suggests that clumps formed at $E \leq 130$ keV will be lost outside the confinement region. The correlation analysis of the SLIP signals with the magnetic probe signal indicated noticeable coherence in a wide range of pitch angles and energies of the lost energetic ions: $\chi = 20^\circ$ – 60° and $E = 20$ – 190 keV. In particular, the highest coher-

ence was observed near the energy ranges of $v_{b\parallel}/v_A \approx 1$ (fundamental excitation of a TAE) and $\sim 1/3$ (side band excitation) [46]. This suggests that strong resonant interaction between TAEs and energetic ions occurs at these energy ranges. The TAE-induced loss flux increases nearly quadratically with increase in the TAE magnetic fluctuation amplitude, suggesting a diffusive type of transport. Here, the magnetic fluctuation amplitude is evaluated at the magnetic probe position. Multiple resonant interactions between energetic ions and AEs in phase space are thought to be a possible candidate mechanism for the diffusive loss, as suggested by AUG tokamak results [61]. Moreover, the dependence of the TAE-induced losses on the TAE amplitude was studied in the LHD by scanning the magnetic axis position. The TAE-induced loss fluxes exhibited quadratic or stronger dependences on the TAE amplitude when the magnetic axis position was shifted outward. Note that the helical field ripple becomes large in outward-shifted LHD plasmas. A numerical simulation using a guiding center orbit code for the plasma region and a full orbit code for the region outside the plasma showed qualitative agreement with the results of the above-mentioned plasma position scan experiments [62]. Although the observed loss characteristics may be explained by multiple resonance interactions, as discussed for tokamaks, helical field ripple in LHD plasmas may also play an important role in the TAE-induced losses. The loss mechanisms in the LHD having a 3D magnetic configuration are still unclear and are under investigation.

In many tokamaks, energetic ion loss and/or redistribution induced by AEs are routinely monitored by neutron detectors. $D\alpha$ emission by energetic ions was successfully measured in DIII-D, and the radial profiles of confined energetic ions were derived from the data. The experimental results showed that the RSAE and C-TAE modes redistributed energetic ions and led to a noticeably flat profile of energetic ion density in the plasma core region [63]. Convective and diffusive types of energetic ion losses by AEs were studied by a scintillator probe in AUG [61]. Single TAEs and RSAEs cause convective loss, and overlapping of a TAE and RSAE causes diffusive loss. Even a single TAE causes diffusive loss if the TAE amplitude exceeds a certain threshold.

5. Summary and Future Issues

We outlined recent research progress in interactions between energetic ions and MHD waves such as shear Alfvén waves in the LHD compared with those in tokamak plasmas. The key results are summarized as follows: (1) TAEs are commonly observed in LHD plasmas with finite magnetic shear as same as tokamak plasmas. In LHD plasmas with a large field period number ($N = 10$), TAEs show the same characteristics as those in a tokamak plasma because the toroidal mode coupling effect is very weak for the TAEs. The detailed differences between the TAE char-

acteristics in LHD and tokamak plasmas arise from the differences in the $1/2\pi$ profile shape. RSAEs in RS plasmas in the LHD have the same characteristics as those in tokamak RS plasmas but show a different frequency sweeping caused by the different sign of the curvature of the q profile $q''(\rho_o)$, that is, $q''(\rho_o) < 0$ in the LHD and $q''(\rho_o) > 0$ in a tokamak. Moreover, it is also strongly affected by the fact that the observed RSAE in the LHD plasma with a large counter NB driven current is a negative frequency mode propagating in the electron diamagnetic drift direction which will be caused by the anisotropic velocity distribution function of energetic ions. (2) Energetic-ion-driven GAMs were observed in RS plasmas in the LHD, as in a tokamak. This is an interesting mode that may play an important role in flow generation and bulk ion heating. This mode can be destabilized owing to the anisotropic velocity distribution function of energetic ions. (3) TAE bursts induce redistribution and/or losses of energetic ions in LHD plasmas heated by tangential NBI, similar to the case for tokamak plasmas.

Important research areas that have not yet been intensively explored in the LHD are the following:

- (i) Characterization of low-frequency energetic-ion-driven modes of which the gaps are generated by acoustic Alfvén wave coupling, for instance, beta-induced Alfvén eigenmodes (BAEs) [64],
- (ii) Excitation of low-frequency energetic-ion-driven modes such as fishbone instabilities by trapped energetic ions,
- (iii) MHD spectroscopy, which is aimed at extracting accurate information on MHD equilibrium, such as the rotational transform profile and electron/ion temperature, based on the linear and nonlinear characteristics of various energetic-ion-driven AEs (TAEs, RSAEs, BAEs, HAEs, and so on) and GAM [3],
- (iv) Improvement in bulk plasma confinement and energy channeling to the bulk plasma by energetic-ion-driven modes such as AEs and GAM [3, 50],
- (v) Study of energetic ion transport by various energetic-ion-driven modes in the regime where energetic ions have a small gyro-radius and near isotropic velocity distribution toward a fusion reactor, and
- (vi) Effects of micro-turbulence on slowed-down energetic ions.

Acknowledgments

The author acknowledges the LHD experiment team at NIFS, in particular K. Ogawa, M. Isobe, M. Osakabe, T. Tokuzawa, K. Ida, T. Ido, A. Shimizu, S. Morita, K. Nagaoka, and K. Narihara, for their support on this research. He also thanks D. A. Spong (ORNL), N. Nakajima (NIFS), Y. Todo (NIFS), F. Watanabe (Kyoto Univ.), S. Yamamoto (Kyoto Univ.), C. Nührenberg (IPP, Greifswald), M. Takechi (JAEA), G. Matsunaga (JAEA), K. Shinohara (JAEA), and S. Sharapov (CCFE) for their sup-

port. This work was supported in part by Grants-in-Aid for Scientific Research from MEXT (No. 16082209) and from JSPS (No. 12480127, No. 16656287, No. 21360457, and No. 24360386), and the LHD project budget (NIFS09ULHH508). This research was also supported by the JSPS-CAS Core University Program in the field of Plasma and Nuclear Fusion.”

- [1] A. Fasoli, C. Gormenzano, H.L. Berk *et al.*, Nucl. Fusion **47**, S264 (2007).
- [2] L.P. Ku *et al.*, Fusion Sci. Technol. **54**, 673 (2008).
- [3] K. Toi, K. Ogawa, M. Isobe, M. Osakabe, D.A. Spong and Y. Todo, Plasma Phys. Control. Fusion **53**, 024008 (2011).
- [4] C. Schwab, Phys. Fluids B **5**, 3195 (1993).
- [5] N. Nakajima, C.Z. Cheng and M. Okamoto, Phys. Fluids B **4**, 1115 (1992).
- [6] Ya. I. Kolesnichenko and V.V. Lutsenko, H. Wobig, Yu. V. Yakovenko and O.P. Fesenyuk, Phys. Plasmas **8**, 491 (2001).
- [7] D.A. Spong, R. Sanchez and A. Weller, Phys. Plasmas **10**, 3217 (2003).
- [8] S. Yamamoto, K. Toi, S. Ohdachi, N. Nakajima, S. Sakakibara *et al.*, Nucl. Fusion **45**, 326 (2005).
- [9] K. Toi, M. Takechi, M. Isobe, N. Nakajima, M. Osakabe *et al.*, Nucl. Fusion **40**, 1349 (2000).
- [10] M.N. Rosenbluth, H.L. Berk, J.W. Van Dam and D.M. Lindberg, Phys. Fluids B **4**, 2189 (1992).
- [11] H.L. Berk, J.W. Van Dam, Z. Guo and D.M. Lindberg, Phys. Fluids B **4**, 1806 (1992).
- [12] F. Zonca and L. Chen, Phys. Rev. Lett. **68**, 592 (1992).
- [13] D.A. Spong, E.D’Azevedo and Y. Todo, Phys. Plasmas **17**, 022106 (2010).
- [14] M. Takechi, K. Toi, S. Takagi *et al.*, Phys. Rev. Lett. **83**, 312 (1999).
- [15] K. Toi, S. Yamamoto, N. Nakajima, S. Ohdachi, S. Sakakibara *et al.*, Plasma Phys. Control. Fusion **46**, S1 (2004).
- [16] Ya.I. Kolesnichenko, S. Yamamoto, K. Yamazaki, V.V. Lutsenko, N. Nakajima *et al.*, Phys. Plasmas **11**, 158 (2004).
- [17] G.Y. Fu, C.Z. Cheng, R. Budny, Z. Cheng, D.S. Darrow *et al.*, Phys. Rev. Lett. **75**, 2336 (1995).
- [18] M. Saegusa *et al.*, Plasma Phys. Control. Fusion **37**, 295 (1995).
- [19] S.E. Sharapov *et al.*, Nucl. Fusion **39**, 373 (1999).
- [20] G.J. Kramer, S.E. Sharapov, R. Nazikian, N.N. Gorelenkov and R.V. Budny, Phys. Rev. Lett. **92**, 015001 (2004).
- [21] Ya. I. Kolesnichenko *et al.*, Phys. Plasmas **14**, 102504 (2007).
- [22] B.N. Breizman, H.L. Berk, M.S. Pekker, S.D. Pinches and S.E. Sharapov, Phys. Plasmas **10**, 3649 (2003).
- [23] H.L. Berk, D.N. Borba, B.N. Breizman *et al.*, Phys. Rev. Lett. **87**, 185002 (2001).
- [24] S.E. Sharapov, B. Alper, H.L. Berk, D.N. Borba, B.N. Breizman *et al.*, Phys. Plasmas **9**, 2027 (2002).
- [25] S.E. Sharapov *et al.*, Nucl. Fusion **46**, S868 (2006).
- [26] H. Kimura, S. Moriyama, M. Saigusa, Y. Kusama, T. Ozeki *et al.*, in *Fusion Energy 1996*, Proceedings of the 16th International Conference, Montreal, 1996 (IAEA, Vienna, 1997), Vol. 3, p. 295.
- [27] M. Takechi, A. Fukuyama, M. Ishikawa *et al.*, Phys. Plasmas **12**, 082509 (2005).
- [28] M. Van Zeeland *et al.*, Nucl. Fusion **46**, S880 (2006).
- [29] J.A. Snipes, N. Basse, C. Boswell, E. Edlund, A. Fasoli *et al.*, Phys. Plasmas **12**, 056102 (2005).
- [30] N.A. Crocker, E.D. Fredrickson, N.N. Gorelenkov *et al.*, Phys. Plasmas **15**, 102502 (2008).
- [31] S.D. Pinches *et al.*, 2006 Proc. 21st Int. Conf. Fusion Energy 2006 (Chengdu, 2006) (Vienna: IAEA) CD-ROM file EX/7-2Ra and <http://www-naweb.iaea.org/naweb/physics/fec/fec2006/html/index.htm>
- [32] H.L. Berk, C.J. Boswell, D. Borba *et al.*, Nucl. Fusion **46**, S888 (2006).
- [33] R. Nazikian, G.Y. Fu, M.E. Austin, H.L. Berk, R.V. Budny *et al.*, Phys. Rev. Lett. **101**, 185001 (2008).
- [34] G.Y. Fu, Phys. Rev. Lett. **101**, 185002 (2008).
- [35] B.N. Breizman, Proc. Theory of Fusion Plasmas: Joint Varenna-Lausanne International Workshop (Varenna, Italy, 2006) CP871.
- [36] G.Y. Fu and H.L. Berk, Phys. Plasmas **13**, 052502 (2006).
- [37] K. Toi, F. Watanabe, T. Tokuzawa, K. Ida, S. Morita *et al.*, Phys. Rev. Lett. **105**, 145003 (2010).
- [38] K. Toi *et al.*, “Alfvén Eigenmodes and Geodesic Acoustic Modes Driven by Energetic Ions in an LHD Plasma with Non-monotonic Rotational Transform Profile”, 22th IAEA Fusion Energy Conference 13-18 Oct. 2009, Geneva, Switzerland. Paper No.EX/P8-4.
- [39] K. Toi, M. Isobe, M. Osakabe, K. Ogawa, D.A. Spong, Y. Todo, Contrib. Plasma Phys. **50**, 493 (2010).
- [40] K. Toi, F. Watanabe, T. Tokuzawa, A. Shimizu, T. Ido *et al.*, “Nonlinear Interaction between Alfvén Eigenmode and Geodesic Acoustic Mode Excited by Energetic Ions in the Large Helical Device”, European Conference Abstracts, 35th EPS Plasma Physics Conference, 9-13 June 2008, Crete, Greece, Paper No. P1.054.
- [41] D.A. Spong *et al.*, “Energetic Particle Physics Issues for three-dimensional toroidal configurations”, Proc. 21th IAEA FEC, 2008, Geneva, paper No.TH/3-4.
- [42] H. Sugama and T.H. Watanabe, Phys. Plasmas **13**, 012501 (2006).
- [43] T. Watari *et al.*, Phys. Plasmas **13**, 062504 (2006).
- [44] H.V. Wong *et al.*, Phys. Lett. A **251**, 126 (1999).
- [45] S. Yamamoto, K. Toi, N. Nakajima, S. Ohdachi, S. Sakakibara *et al.*, Phys. Rev. Lett. **91**, 245001 (2003).
- [46] K. Ogawa, M. Isobe, K. Toi, F. Watanabe, D.A. Spong, A. Shimizu, M. Osakabe *et al.*, Nucl. Fusion **50**, 084005 (2010).
- [47] K. Toi *et al.*, “Characteristics of Energetic-Ion-Driven Geodesic Acoustic Modes in the Large Helical Device (LHD)”, 12th IAEA TM on Energetic Particles in Magnetic Confinement Systems, 7-10 Sep. 2011, Austin, USA, Paper No. O-4.
- [48] T. Ido *et al.*, Nucl. Fusion **51**, 073046 (2011)
- [49] T. Ido *et al.*, “Potential fluctuation of energetic particle induced geodesic acoustic mode in the Large Helical Device”, 18th International Stellarator/Heliotron Workshop, 29 Jan.-3 Feb., 2012, Canberra, Australia, Paper No. S15-1.
- [50] M. Osakabe *et al.*, “Effect of energetic-particle induced n=0 instabilities to bulk-ions on LHD”, 12th IAEA TM on Energetic Particles in Magnetic Confinement Systems, 7-10 Sep. 2011, Austin, USA, Paper No. O-3.
- [51] W.W. Heidbrink, Phys. Plasmas **15**, 055501 (2008).
- [52] Ya.I. Kolesnichenko *et al.*, Plasma Phys. Control. Fusion **53**, 024007 (2011).
- [53] H.L. Berk, B.N. Breizman and M. Pekker, Phys. Rev. Lett. **76**, 1256 (1996).

- [54] A. Fasoli, B.N. Breizman, D. Borba *et al.*, Phys. Rev. Lett. **81**, 5564 (1998).
- [55] R.E. Heeter, A.F. Fasoli and S.E. Sharapov, Phys. Rev. Lett. **85**, 3177 (2000).
- [56] M.K. Lilley, B.N. Breizman and S.E. Shrapov, Phys. Rev. Lett. **102**, 195003 (2009).
- [57] M. Osakabe, S. Yamamoto, K. Toi, Y. Takeiri, S. Sakakibara *et al.*, Nucl. Fusion **46**, S911 (2006).
- [58] M. Osakabe *et al.*, “Enhanced Radial Transport of Energetic Particles with Alfvén Eigen mode on LHD”, 9th IAEA Technical Meeting on Energetic Particles in Magnetic Confinement Systems, 9-11 November 2005, Takayama, Japan, Paper No. IT-03.
- [59] M. Osakabe *et al.*, “Clump and Hole formation in the energetic particle spectra by the toroidicity induced Alfvén Eigenmodes and their behaviors during the mode activities”, 11th IAEA Technical Meeting on Energetic Particles in Magnetic Confinement Systems, 21-23 Sep., 2009, Kiev, paper no: IT-5.
- [60] Y. Todo, N. Nakajima, M. Osakabe *et al.*, J. Plasma Fusion Res. **3**, S1074 (2008).
- [61] M. García-Muñoz *et al.*, Phys. Rev. Lett. **104**, 185002 (2010).
- [62] K. Ogawa, M. Isobe, K. Toi, D.A. Spong, M. Osakabe *et al.*, Nucl. Fusion **52**, 094013 (2012).
- [63] W.W. Heidbrink, M.A. Van Zeeland, M.E. Austin, K.H. Burrell, N.N. Gorelenkov *et al.*, Nucl. Fusion **48**, 084001 (2008).
- [64] D.A. Spong, B.N. Breizman, D.L. Brower, E.D’Azevedo, C.B. Deng *et al.*, Contrib. Plasma Phys. **50**, 708 (2010).